Dispersion Elimination and Harmonic Behavior in Optical Networks

Eszter Udvary, *Member, IEEE,* Attila Hilt, *Member, IEEE,* Tibor Berceli, *Fellow, IEEE*

***Abstract*—Eliminating dispersion effects fast is a crucial concern when building next generation optical networks. Dispersion penalty has been investigated widely in 1550nm fiber-optical links transmitting different kind of signals. However, only a few papers addressed the harmonics generation effect. This paper presents theoretical and experimental results on the estimation of harmonic effects in the transmission. An approach is presented in this paper to overcome the radio frequency carrier suppression, based on the joint effect of SOA chirp, chromatic dispersion and nonlinearities in optical link. The frequency notches caused by the dispersion-induced carrier suppression effect may be sharply alleviated and the performance of the transmitted digital signal can be improved. The saturated SOA also affects the level and nature of harmonics.**

***Index Terms*—Dispersion media, Distortion, Intensity modulation, Optical fiber, Semiconductor Optical Amplifier, Subcarrier multiplexing**

I. Introduction

THE optical fiber is more and more employed all the way into the home to enable fast connection. The transmission of optical signals in an optical communication system using standard single mode optical fiber near 1550nm may be limited by optical effects such as chromatic dispersion. Dispersion, like attenuation, is an impairment that degrades the optical signal as it travels over distance. It is a physical phenomenon caused by the fact that the various frequencies have different propagation velocities.

This limitation mainly is caused by the radio-frequency (RF) carrier suppression effect due to dispersion-induced sideband cancellations at certain combinations of microwave frequencies and propagation distances.

On the other hand the optical signals may be transmitted as pulses of light in an optical fiber. When light propagating within an optical fiber undergoes chromatic dispersion, the light is delayed within the optical fiber. Propagation delay leads to spreading of the light pulses, which may affect the performance of the system. The specific amount of dispersion that an optical signal undergoes varies depending upon the wavelength of the optical signal. The extent to which dispersion varies as a function of light wavelength is often referred to as dispersion slope.

To our knowledge the first theoretical treatment of the problem was published by [1] and experimentally demonstrated by [2].

Various dispersion management techniques have been used to reduce dispersion and to manage dispersion slope by reducing dispersion at individual channel wavelengths. One dispersion management technique involves dispersion mapping where optical fiber types are selected and arranged to manage the dispersion as a function of distance in the transmission segments of an optical communication system. Another solution, the pre-distortion of the signal is a mature field within signal processing and many different adaptive equalization algorithms and architectures have been studied [3, 4].

Different technical solutions have been proposed using standard optical fiber such as optical single sideband (SSB) modulation [5, 6], chirped fiber gratings [7], variable chirp in electroabsorption modulators [8], self-phase modulation effect introduced by the fiber [9], dual mode lasers [10], special Mach–Zehnder EOM [11], midway optical phase conjugation, etc.

Dispersion management is particularly important in wavelength division multiplexed (WDM) optical communication systems transmitting multiple channels at multiple wavelengths.

In this paper, two approaches to overcome dispersion-induced effects based on fiber nonlinearities and adjusting the chirp and phase modulation generated by saturated semiconductor optical amplifiers (SOAs) are investigated. The results show that the fading of the RF-to-RF system response can be significantly alleviated. As the SOA input power increases (the device goes to saturation region) or the operation point (bias current) increases the frequency notches of the RF response are shifted to higher frequencies and further reduced.

II. Chromatic Dispersion Penalty

A. Optical transmissions of microwave signals

Optical Intensity Modulation (IM) generates optical double sidebands (DSB). When DSB signal propagates over the fiber a phase difference is observed between the two sidebands due

Manuscript received February 20, 2008. This work was supported in part by the Hungarian Scientific Research Fund (OTKA) and the IST-ISIS European Union Network of Excellence project.

Eszter Udvary and Tibor Berceli are with Budapest University of Technology and Economics, Department of Broadband Infocommunication Systems, H-1111 Budapest, Goldmann György tér 3, Hungary (phone.: (+36)-1-463-2634, fax: (+36)-1-463-3289, e-mail: udvary@mht.bme.hu).

Attila Hilt is with Network Planning and Optimization (NPO, WSE, CE) Nokia Siemens Networks Magyarország Kft., H-1092 Budapest, Köztelek utca 6., Hungary (e-mail: attila.hilt@nsn.com)

to the chromatic dispersion.

The frequency transfer function of the optical link can be written:

$$H_{link}(f) = \cos\left(\frac{\lambda^2 \cdot D \cdot \pi \cdot f^2 \cdot L}{c}\right) \quad (1)$$

Where D is the fiber dispersion parameter, L is the fiber length, f is the modulation frequency, c is the light speed in vacuum, λ is the operating wavelength. For simplicity the linear loss and delay of the fiber are neglected in eq.1. So, repetitive reduction of the received RF carrier power is observed as shown in Fig.1.

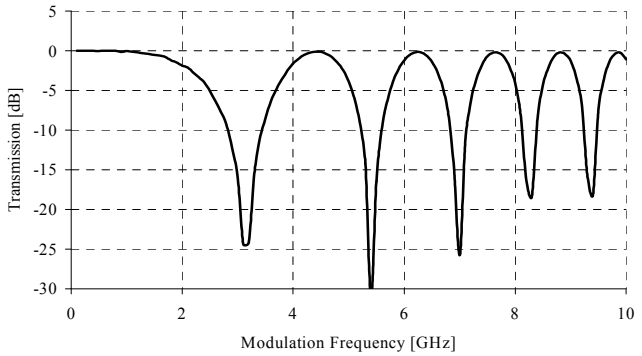

Fig. 1. Simulated results, dispersion penalty over 400km fiber

Using directly modulated laser diodes or unbalanced external modulator the maximum link length or maximum RF bandwidth is expected to be much smaller due to the positive chirping of the optical transmitter (Fig.2) [12].

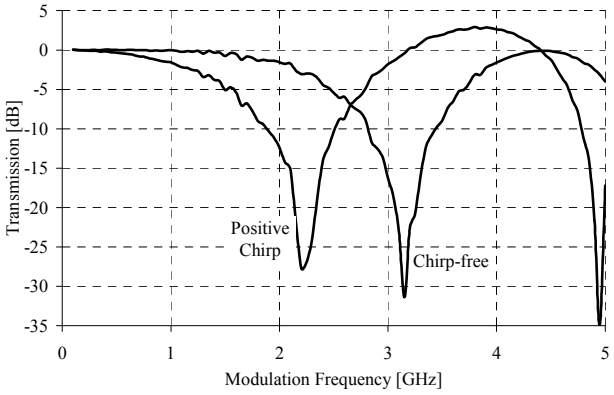

Fig. 2. Simulated results, positive transmitter chirp decreases the maximum modulation bandwidth

B. Optical transmission of baseband digital signals

The dispersion limit for about 1 dB optical power penalty is estimated by [13]

$$B = \sqrt{\frac{c}{2 \cdot \lambda^2 \cdot D \cdot L}} \quad (2)$$

If the dataspeed is lower, the data transmission is limited by the optical signal-to-noise ratio. In case of higher data speeds dispersion compensation techniques will be necessary.

The baseband bit error rate (BER) in a dispersion limited system deteriorates versus the fiber length and data speed. In a practical system the fiber length is not a free parameter, hence the required BER determines the applicable modulation bandwidth. Fig.3. shows the simulated BER versus data speed for different fiber lengths. The plotted results were simulated by VPI software [14].

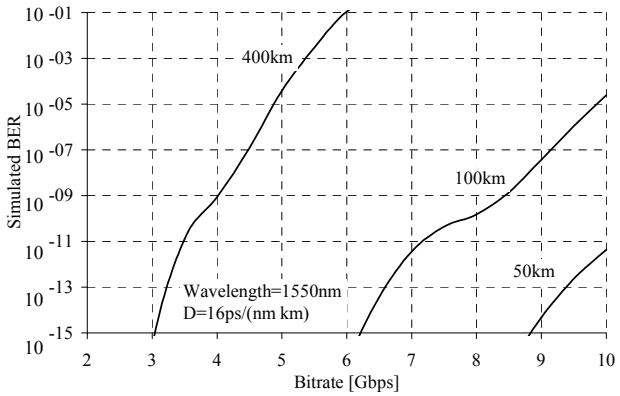

Fig. 3. Simulated BER versus data speed for different links

Fig.4. represents the baseband eye diagram degradation assuming a chirp-free transmitter. The effect of the transmitter chirp can be demonstrated by the eye diagram and BER degradation, too. Fig.5 shows the eye diagram of 2.5Gbit/s baseband data with positive chirp transmitter. Same time the BER increases from 10^{-25} to 10^{-11} value due to the positive chirp of the transmitter.

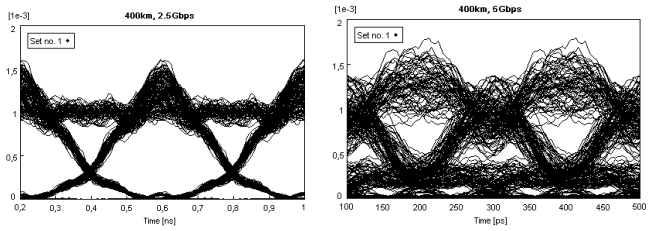

Fig. 4. Simulated eye diagrams at output (400km) for 2.5 and 5 Gbit/s, chirp-free transmitter

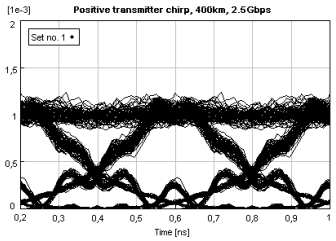

Fig. 5. Simulated eye diagrams at output (400km) for 2.5 Gbit/s, Positive transmitter chirp

III. FIBER NONLINEARITIES

With the increase of input optical power provided by high intensity laser diodes (LD), non-linearity of optical fiber can no longer be neglected. At a given density of photon flux self-phase modulation (SPM) can become significant and one must consider the distortions caused by SPM during the design process of microwave (MW) optical systems. High input intensity modifies the transfer function of the fiber and can

compensate modulation suppression caused by dispersion [15]. As the signal intensity increases the notches caused by dispersion shift to higher modulation frequencies (Fig.6. and Fig.7). The measurement and simulation results show that the fiber-induced SPM less influences of the frequency notches in case of relatively low optical power.

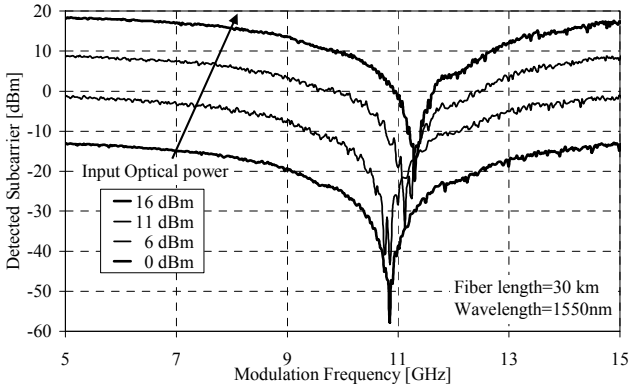

Fig. 6. Measurement results over 30 km fiber at four different average input intensities

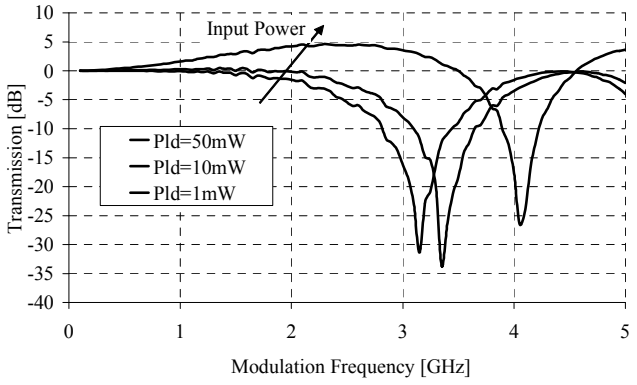

Fig. 7. Simulation results over 400km fiber at different average input

IV. HARMONICS GENERATION

A. Coherent model of optical IM/DD transmission

In the analysis usually an approximated case of only three spectral lines of optical field $E_{opt}(\omega)$ is assumed at the fiber input. This simplification reduces significantly the calculation difficulties. In the general case however, several optical field spectral lines are present at the fiber input. At the detection side amplitude and phase of these optical field spectral components are determined by the optical transmitter (LD or external modulator) as well as by parameters of propagation in the dispersive fiber. In coherent models the calculation is based on the optical field and not on the optical intensity. Only coherent models can explain properly the exact detected levels of different harmonics of the microwave modulation signal. In this paper based on the coherent model of the microwave optical link we simulate the effect of chromatic dispersion in the general case of several spectral lines. For simplicity fiber birefrigence is neglected [16].

The optical field at the output of the single-frequency modulated laser diode is written as :

$$E(t) = E_0\sqrt{1+m\cos(\omega_{RF}t)}\,e^{j\{\omega_{opt}t+\beta\cos[\omega_{RF}t+\theta]+\phi(t)\}} \quad (3)$$

where β is the usual frequency modulation (FM) index, $\phi(t)$ is the phase noise term and θ is the phase delay between AM and FM. Its typical value is between 0 and $-\pi/2$. Usually Eq.1 is simplified as [17]:

$$E(t) = E_0\sqrt{1+m\cos(\omega_{RF}t)}\,e^{j\{\omega_{opt}t+\beta\sin[\omega_{RF}t+\theta_a(\omega_{RF},I_0)]\}} \quad (4)$$

where θ_a is the phase lag in addition to $\pi/2$. As indicated, θ_a is frequency and optical power dependent.

In the case of external modulation by a dual-electrode interferometer the optical field is:

$$E(t) = \frac{E_o}{2}\left(\cos(\omega_o t+\gamma_1\pi+\alpha_1\pi\cos\omega_{RF1}t)+ \right. \\ \left. +\cos(\omega_o t+\gamma_2\pi+\alpha_2\pi\cos(\omega_{RF2}t+\theta_{RF}))\right) \quad (5)$$

where θ_{RF} represents the phase difference between the driving RF signals of the two electrodes. γ_i and α_i are the normalized DC and RF voltages driving the modulator arms, respectively. The optical field in frequency domain is expressed by Fourier transform of the field given in time domain. The output optical field at the fiber end is calculated as:

$$E_{opt,out}(\omega_{opt}) = E_{opt,in}(\omega_{opt})A(L)e^{-j\beta(\omega_{opt})L} \quad (6)$$

where L is the fiber length and $\beta(\omega)$ is the propagation factor. Using Fast Fourier Transformation (FFT) we can calculate the output optical field. Due to quadratic photodetection, the current of an ideal photodetector (PD) is proportional to the optical intensity[18].

$$i_{PD}(t) = R_{PD}\langle E(t)\,E^*(t)\rangle \quad (7)$$

< > means time averaging taken over a few optical periods. Time averaging means the physical fact, that the PD cannot response to rapid changes at optical frequencies, only the MW/MMW modulation envelope of the optical carrier is detected. The general coherent model is shown in Fig.8. [19].

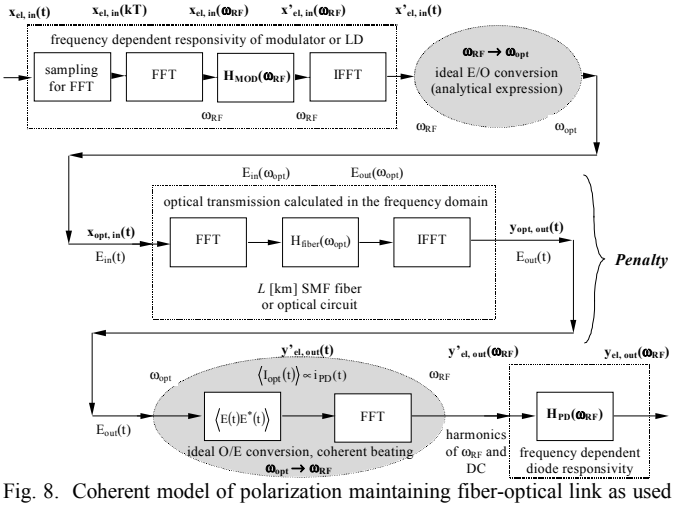

Fig. 8. Coherent model of polarization maintaining fiber-optical link as used in our computer simulations

B. Experimental and theoretical results

Detected levels of fundamental, second and third harmonics of the optically transmitted MW signals have been measured.

The frequency of the signal source modulating the optical transmitter and the center frequency of the spectrum analyzer have been set simultaneously by a measurement control and data acquisition software [20]. Several different fiber lengths have been tested. Fig.9 and 10 show the levels measured and simulated over a 50 km long fiber, respectively. In the simulation the finite spectral purity of the signal source (multitone modulation at the MZM) was considered, hence the MZM driving electrical signal itself was composed of three tones, the fundamental and its 2nd and 3rd harmonics. A further investigation in the depth of modeling as well as in the measurement procedure is possible. Effects of polarization state between the optical source and the MZM, polarization mode dispersion, or more accurate calibration in the measurements can be determined.

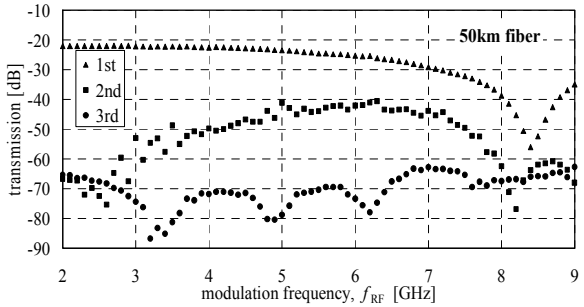

Fig. 9. Measured levels of fundamental, second and third harmonics. L=50 km

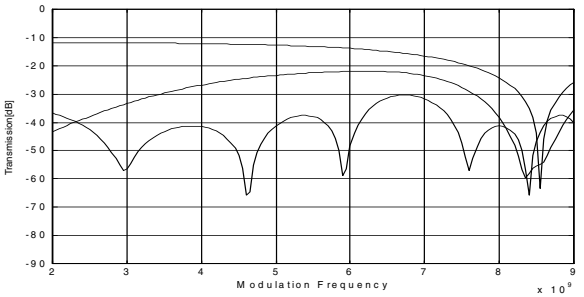

Fig. 10. Simulated results for L=50 km long fiber. (push-pull MZM, γ=0.5, α=0.4, A_{f2}/A_{f1}=0.07, A_{f3}/A_{f1}=0.05, D=17ps/km/nm)

V. SOA Based Dispersion Compensation

When the incoming optical power of the laser amplifier is intensity modulated, the optical gain is affected in both magnitude and phase via the modulation of the complex refractive index caused by the electron density. Consequently, in SOA the optical signal becomes amplitude modulated (AM) and phase modulated (PM) caused by carrier density change. It is fundamental to know the behavior of the refractive index within the active region. It can be modeled using the Linewidth Enhancement Factor (*LEF*=Henry factor= α factor) approximation. Measurements of *LEF* can be found in the literature and have shown that *LEF* is not a mere constant factor, but it is for instance a function of bias current, wavelength and input optical power. In the unsaturated region the *LEF* value ranges from 2 to 7 for GaAs and GaInAsP conventional lasers and from 1.5 to 2 for quantum well lasers [12,21]. However, as the optical input power (P_{in}) increases, carrier depletion occurs in SOA and this induces gain saturation. In optical amplifiers under saturation conditions, an increasing input intensity causes a decrease in the amplifier gain (dG/dPin<0). In this case *LEF* can be calculated from the unsaturated LEF value (*LEFunsat*) [21]:

$$\mathrm{LEF} = \mathrm{LEF}_{\mathrm{unsat}} \cdot \frac{\mathrm{dG}}{\mathrm{dP}_{\mathrm{out}}} = \mathrm{LEF}_{\mathrm{unsat}} \cdot \frac{\mathrm{dG}/\mathrm{dP}_{\mathrm{in}}}{1+(\mathrm{dP}_{\mathrm{out}}/\mathrm{dP}_{\mathrm{in}})} \tag{8}$$

Where G is the optical gain, P_{in} is the input average optical power and P_{out} is the output average optical power.

The chirping parameter which is positive for light sources and unsaturated optical amplifiers is negative for saturated amplifiers [22]. Fig.11. represents the optical gain and approximately the *LEF* dependence on the optical power. When the input power becomes larger than the saturation value, the chirp parameter rapidly falls to a negative value. However it depends on the wavelength with which the SOA gain is compressed.

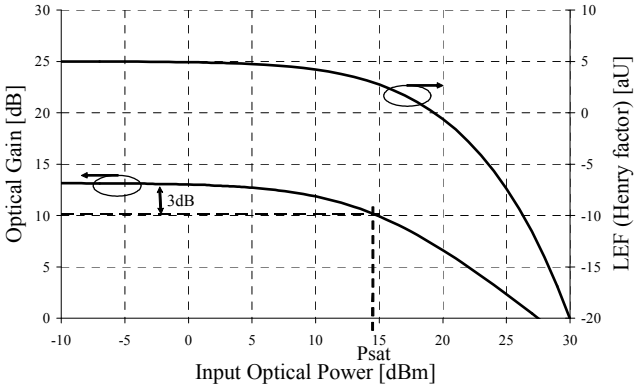

Fig. 11. Optical gain saturation and the calculated chirp

The negative chirp of saturated SOA cancels the positive chirp-parameter of modulator, in such way enhances the transmission distance and operating frequency. Furthermore the optical amplification causes RF signal gain, too [23]. However the SOA adds significant noise to the system. The negative chirp affects both sidebands and then causes the asymmetrical optical power between sidebands [24]. As a result, the RF carrier suppression effect is reduced. The frequency transfer function between the intensity modulations at the input and output can be written:

$$\begin{aligned} \mathrm{H}_{\mathrm{SOA+link}}(\mathrm{f}) = &\cos\left(\frac{\lambda^2 \cdot \mathrm{D} \cdot \pi \cdot \mathrm{f}^2 \cdot \mathrm{L}}{\mathrm{c}}\right) - \\ &- \mathrm{LEF} \cdot \sin\left(\frac{\lambda^2 \cdot \mathrm{D} \cdot \pi \cdot \mathrm{f}^2 \cdot \mathrm{L}}{\mathrm{c}}\right) + \\ &+ \mathrm{j} \cdot \mathrm{LEF} \cdot \frac{\mathrm{f_c}}{\mathrm{f}} \cdot \sin\left(\frac{\lambda^2 \cdot \mathrm{D} \cdot \pi \cdot \mathrm{f}^2 \cdot \mathrm{L}}{\mathrm{c}}\right) \end{aligned} \tag{9}$$

The calculated RF responses of 400 km fiber for different chirp parameters of the optical amplifier are depicted in Fig.12. All the results have been calculated for an optical input

power of 0 dBm in order to reduce the influence of the nonlinear effects at the fiber. By comparing the results to the reference case of a zero-chirp situation (*LEF*=0), for *LEF*>0, the bandwidth of the system is reduced, while for *LEF*<0, the achievable bandwidth increases.

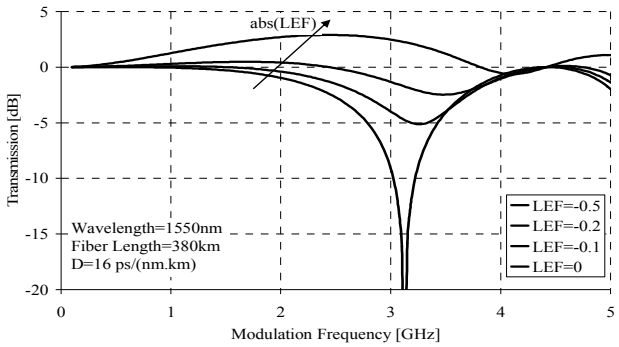

Fig. 12. Calculated RF responses of the optical link for different SOA chirp parameters

Experimental work was executed in the laboratory over different length of singlemode fibers. Fig13. shows the simplified measurement setup. The SOA under test was driven by different bias (DC) currents. The polarization state of the incoming optical power was optimized by polarization controller. The harmful effect of the optical reflection was eliminated by optical isolators. The required optical power and wavelength were produced by a tunable laser source. The intensity modulated optical signal was detected by a photodetector. The setup was controlled by a computer program, hence the measurement parameters were carefully set by the program and the measurement results were processed and stored.

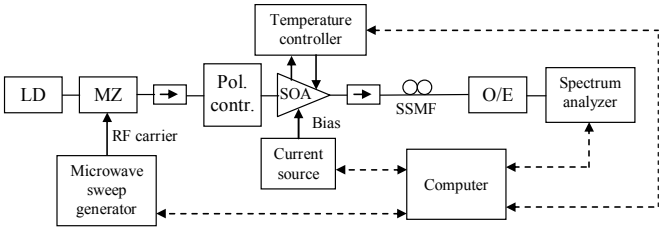

Fig. 13. Simplified experimental setup

The RF response was measured with different parameters (Fig.14). As the SOA bias current (optical gain) increases the frequency notches of the RF response are reduced and shifted to higher modulation frequencies.

Based on the results, we may conclude that the interplay of chirp generated by the saturated SOA and chromatic dispersion enables a significant reduction of the dispersion-induced effect. Introducing the frequency and optical power dependence in the SOA chirp model is required in the future.

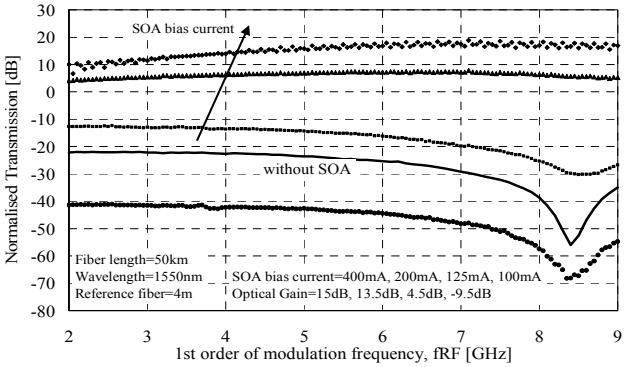

Fig. 14. Measured RF response with SOA, normalized to back-to-back optical link parameters

In radio over fiber systems the radio frequency carrier is modulated by digital information. The above presented dispersion compensation technique affects the eye diagram and the BER of the modulation signal. If the subcarrier frequency is near one of the frequency notches caused by dispersion the eye diagram closes and the communication deteriorates or get lost. Applying the optimized SOA compensator the eye diagram opens and the BER is improved (Fig.15.)

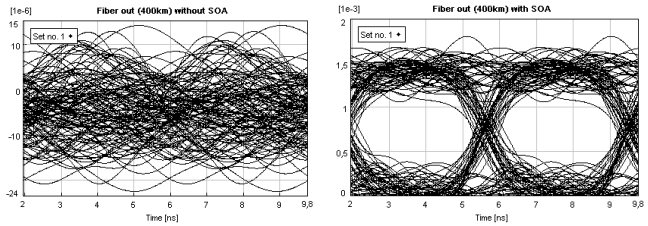

Fig. 15. Simulated eye diagram, 400km optical link, subcarrier frequency is 3.2GHz, modulation bandwidth 512MHz, without and with SOA

VI. Harmonic Generation with SOA

The simulations show the SOA device modifies the harmonic generation, too (Fig.16.). The depths of second order harmonic rejections are not reduced significantly, but their frequencies are shifted. However the rejections of third order harmonic are eliminated. The levels of harmonics were measured with different parameters (Fig.17). As the SOA bias current (optical gain) increases the form of second order response will not change significantly, just the level of the signal will increase, because of the optical gain. Same time the third order product will increase and the frequency notches of the third order harmonic response are reduced and shifted to higher modulation frequencies.

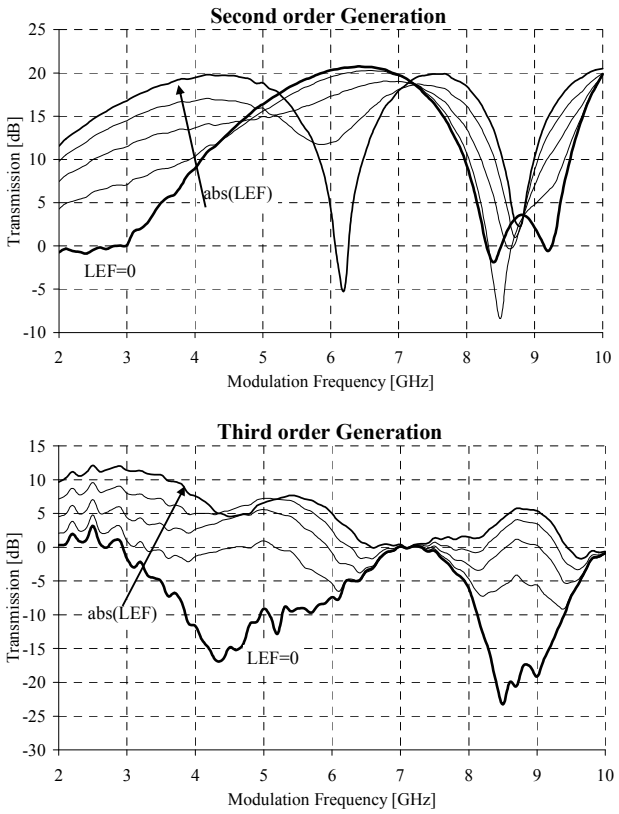

Fig. 16. Simulated results for L=50 km long fiber with different SOA Chirp parameter

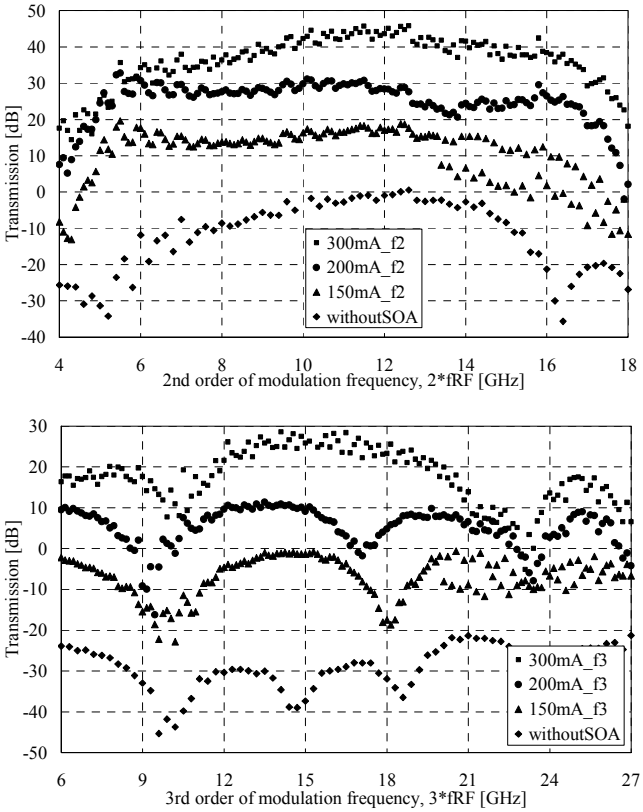

Fig. 17. Measured levels of second and third order harmonics. L=50 km, with different SOA operating point

VII. Conclusion

Compensating dispersion penalty is a key problem when next generation all-optical networks are built. In the paper distortion levels of harmonics have been investigated in fiber-optical transmission of microwave/millimeterwave signals. Second harmonic generation of modulation signals in the optical path has been verified theoretically and experimentally. We presented a general model to calculate harmonic levels and the effect of chromatic dispersion numerically. Levels of detected harmonics are estimated by the developed coherent model. Experimental examples have shown clearly the presence and evolution of harmonics. It was shown that these harmonics also exhibit minima and maxima due to fiber dispersion.

An approach to overcome the RF carrier suppression effect in optical links based on the joint effect of SOA chirp, chromatic dispersion and nonlinearities in optical fiber has been proposed. The experimental and theoretical results show that the frequency notches caused by the dispersion-induced carrier suppression effect may be sharply alleviated and the performance of the transmitted digital signal can be improved.

References

[1] W.van Etten, J.van der Plaats, *Fundamentals of Optical Fiber Communications*, Prentice Hall Int. Series in Optoelectronics, UK, 1991, pp. 62-68

[2] H. Schmuck, "Comparison of optical millimetre-wave system concepts with regard to chromatic dispersion", *Electronics Letters*, Vol.31, No.21, October 1995, pp. 1848-1849

[3] I.Joindot, M.Joindot editors, "Les télécommunications par fibres optiques", *DUNOD et CNET-ENST*, Paris, 1996.

[4] Göran Einarsson : "Principles of Lightwave Communications", *John Wiley & Sons Inc.,* New York, 1996.

[5] G. H. Smith, D. Novak, "Broad-band millimeter-wave (38ghz) fiber-wireless transmission system using electrical SSB modulation to overcome dispersion", *IEEE Photonic Technology Letters*, Vol. 10, No. 1, January 1998, pp. 141-143

[6] J.Park, W.V.Sorin, K.Y.Lau : "Elimination of the Fibre Chromatic Dispersion Penalty on 1550 nm Millimetre-Wave Optical Transmission", *Electronics Letters, Vol.33, No.6, pp.512-513,* 13th March 1997.

[7] J. Marti, J. M. Fuster, R. I. Laming, "Experimental reduction of chromatic dispersion effects in lightwave microwave/millimeter-wave transmission using tapered linearly chirped fiber gratings," *Electronics Lett*ers, vol.33, no.13, 1997

[8] G. H. Smith, D. Novak, "Overcoming chromatic-dispersion effects in fiber-wireless systems incorporating external modulators," *IEEE Trans. Microwave Theory Tech.*, vol.45, Aug. 1997, pp. 1410–1415

[9] V. Polo, J. Marti, F. Ramos, "Mitigation of chromatic dispersion effects employing electroabsorption modulator-based transmitters," *IEEE Photonic Technology Letters*, vol. 11, July 1999, pp. 883–885

[10] D. Wake, C. R. Lima, P. A. Davies, "Optical generation of millimeter-wave signals for fiber-radio systems using a dual-mode DFB semiconductor laser", *IEEE Trans. on Microwave Theory and Techniques*, Vol. 43, No. 9, September 1995, pp. 2270-2276

[11] J. Capmany, D. Pastor, B. Ortega, J. Mora, L. Pierno, M. Varasi, "Theoretical model and experimental verification of 2 x 1 Mach–Zehnder EOM with dispersive optical fiber link propagation", *IEEE Journal of Quantum Electronics*, Vol. 44, Issue 2, February 2008, pp. 165-174

[12] F.Koyama, K.Iga, "Frequency Chirping in External Modulators", IEEE Journal of Lightwave Technology

[13] B. Wedding, B. Franz, B. Junginger, "10-Gb/s optical transmission up to 253 km via standard single-mode fiber using the method of dispersion-supported transmission", *IEEE Journal of Lightwave Technology*, Vol. 12, No. 10, October 1994, pp. 1720-1727

[14] VPI Transmission maker/VPI component maker, user's manual, May 2007

[15] Z. Várallyay, I. Frigyes, O. Schwelb, E. Udvary, L. Jakab, P. Richter, "Soliton propagation of microwave modulated signal through single-mode optical fiber", *Acta Physica Hungarica B) Quantum Electronics*, Akadémiai Kiadó, Volume 23, Numbers 3-4 / November 2005, pp. 175-186

[16] A. Hilt, E. Udvary, T. Berceli, "Harmonic distortion in dispersive fiber–optical transmission of microwave signals", in *Proc. International Topical Meeting on Microwave Photonics MWP2003*, IEEE, Budapest, Hungary, September 10-12, 2003, pp. 151-154.

[17] A. Hilt, "Transmission et traitement optiques des signaux dans les systèmes de télécommunications hertziens", Ph.D. dissertation, Institut National Polytechnique de Grenoble, Grenoble, France, 17. May 1999.

[18] A. Hilt, G. Maury, B. Cabon, A. Vilcot, L. Giacotto, "General approach to chromatic dispersion analysis of microwave optical link architectures", in *Proc. of the 10th Conf. on Microwave Techniques, COMITE'99*, Pardubice, Czech Republic, October 1999, pp. 177-180

[19] A. Hilt, T. Berceli, I. Frigyes, E. Udvary, T. Marozsák, "Fiber-dispersion compensation techniques in optical/wireless systems", in *Proc. 14th International Conference on Microwaves, Radar and Wireless Communications (MIKON2002)*, 20-22 May 2002, Vol.1, pp. 25-36

[20] HP VEE, Hewlett-Packard's visual engineering environment

[21] L. Occhi, L. Schares, G. Guekos, "Phase modeling based on the α factor in bulk semiconductor optical amplifiers", *IEEE Journal of Selected Topics in Quantum Electronics*, 2003, pp. 788-797

[22] T. Watanabe, N. Sakaida, H. Yasaka, F. Kano, M. Koga, "Transmission performance of chirp-controlled signal by using semiconductor optical amplifier", *IEEE Journal of Lightwave Technology*, August 2000, pp. 1069-1077

[23] Sang-Yun Lee, Bon-Jo Koo, Hyun-Do Jung, and Sang-Kook Han, "Reduction of chromatic dispersion effects and linearization of dual-drive Mach-Zehnder Modulator by using semiconductor optical amplifier in analog optical links" in *Proc. ECOC 2002, 28th European Conf. on Optical Communication*, September 8-12, 2002, Copenhagen, Denmark

[24] J. Marti, F. Ramos, J. Herrera, "Experimental reduction of dispersion-induced effects in microwave optical links employing SOA boosters", *IEEE Photonic Technology Letters*, Vol. 13, No. 9, Sept. 2001, pp. 999-1001